

Influence of sawdust on the properties of the ceramic shell used in investment casting process

Sarojrani Pattnaik¹

Received: 1 March 2016 / Accepted: 12 May 2017 / Published online: 26 May 2017
© Springer-Verlag London 2017

Abstract The quality of the investment casting (IC) ceramic shell was enhanced using sawdust as an inexpensive and naturally available additive in the ceramic slurries. The important shell properties such as thickness, porosity, permeability and flexural strength were determined. The ceramic shell accommodated a substantial amount of sawdust because of its low particle density and porous structure which resulted in higher green strength and thickness of the shell. The same shell upon firing led to increased shell porosity and permeability with good knockability characteristic. The addition of sawdust in the secondary layers did not affect the composition of the primary layer of the ceramic shell. The mechanical properties of the aluminium-silicon (Al-Si) alloy castings obtained from the sawdust-modified shells were found to be comparatively higher than those obtained from the conventional shells.

Keywords Ceramic Shell · Casting · Strength · Porosity · Permeability

1 Introduction

IC also known as lost wax, lost pattern and precision casting process is used to manufacture finest quality components which have intricate shapes and thin walls [1]. The surface

texture of the parts produced by the IC process is remarkable. Pattnaik et al. [2] stated some typical applications of the IC process which include manufacture of aircraft engines, airframes, turbine blades, turbocharger wheels, dental parts, etc. The various stages involved in the IC process are creation of disposable wax pattern, construction of ceramic shell around the wax pattern, dewaxing and firing of the ceramic shell and pouring and solidification of the melt inside the ceramic shell followed by knockout operation [3].

The very first stage of the IC process begins with the creation of a wax pattern. The IC waxes are prone to shrinkage. The quality of the wax pattern depends on many process parameters such as the wax composition, injection process parameters, etc. [4]. The author in her previous research had determined the best wax blend composition from cheaply and easily available pattern waxes and determined the optimal input condition using various multi-response optimization techniques such as utility [5], desirability-fuzzy [6] and grey-fuzzy [7] methods. It was found from the previous study that the wax pattern produced at the optimal parametric condition leads to superior IC patterns.

Bonilla et al. [8] used heat transfer-based simulations to determine the injection process parameters so as to forecast the shrinkages occurring in the wax patterns. A technique was further described by Wang et al. [9] to predict the shrinkage of casting based on the deformed CAD model of its corresponding disposable wax pattern. It was found from the numerical simulation and experimental results that the predicted casting shrinkages were only 0.32% lesser than those of the experimental ones. This study shows that the consideration of wax pattern deformation is significant in predicting the investment casting shrinkage.

The second stage of the IC process is the construction of ceramic shell around the wax pattern. The ingredients which are used to prepare the ceramic shells are refractory filler, binder, additives and stucco [10]. The physical characteristics of the

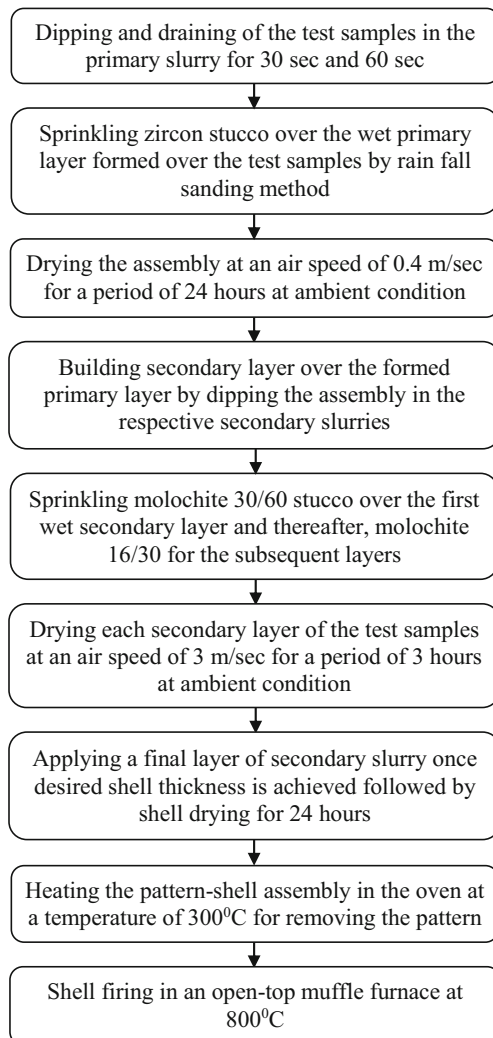
✉ Sarojrani Pattnaik
rani_saroj7@yahoo.co.in

¹ Mechanical Engineering Department, Veer Surendra Sai University of Technology, Burla -768018, India

Table 1 Ingredients to prepare different ceramic slurries

Slurry composition	Primary slurry	Secondary slurry for making a conventional shell	Secondary slurry for making a sawdust-modified shell
Filler (wt%)	Zircon flour –325 mesh	Aluminium-silicate –200 mesh	Aluminium-silicate-200 mesh
Binder (wt%)	Nano-based colloidal silica	Nano-based colloidal silica	Nano-based colloidal silica
Filler loading (kg/kg of binder)	3:1	2:1	2:1
Wetting agent (wt%)	0.3	Nil	Nil
Antifoam (wt%)	0.3	Nil	Nil
Liquid polymer (wt%)	5.0	5.0	Nil
Sawdust particles (wt%)	Nil	Nil	5.0
Deionized water	Approx	Approx	Approx
Stucco	Zircon sand-200 mesh	Molochite 30/60 for secondary-1 Molochite 16/30 for secondary-2 and onwards	Molochite 30/60 for secondary-1 Molochite 16/30 for secondary-2 and onwards

primary slurry influence the surface texture of the investment castings. Ertuan et al. [11] investigated the influence of different

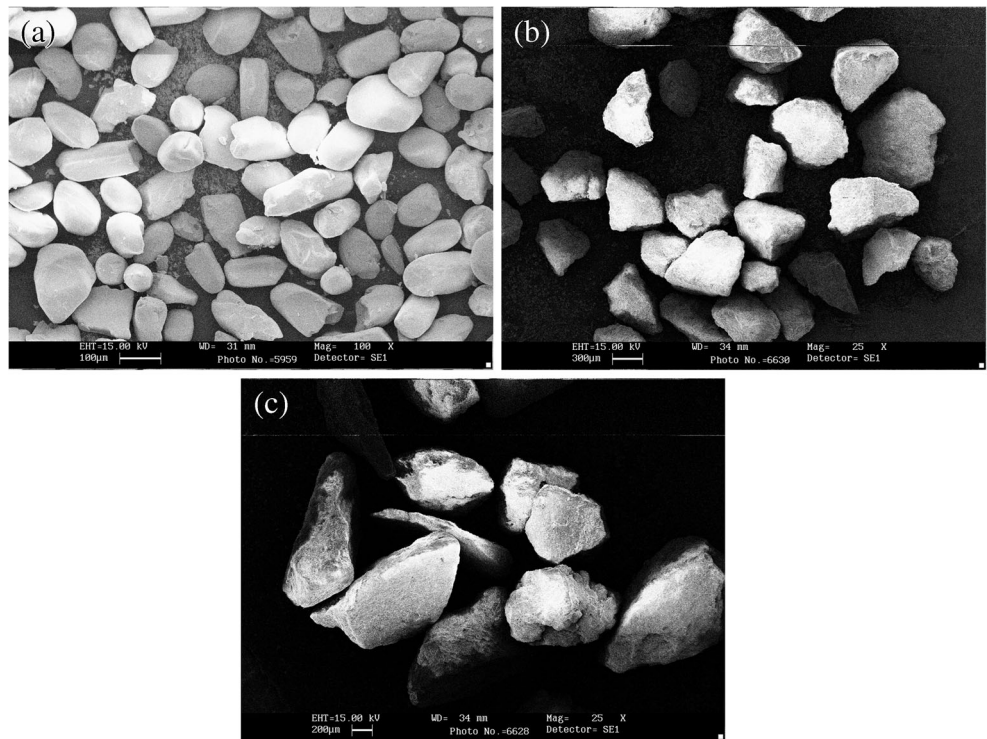
**Fig. 1** Flow chart for building ceramic shell

binders on the physical properties of the primary slurry for titanium alloy investment casting. The results indicated that a highly viscous binder led to increased suspensibility and viscosity of the slurry for the similar powder-to-binder ratio. The primary layer thickness increased with increase in slurry's viscosity.

Jafari et al. [12] investigated on interfacial reaction between in situ melted AZ91D magnesium alloy and ceramic shell of the IC process. It was found that the ceramic shell showed little cracks due to magnesium's high affinity for oxygen gas and involvement of high process temperature, which led to melt penetration through the generated cracks thereby causing adherence of ceramic investments on the cast surface. Liao et al. [13] formed a very smooth thin layer of wax on the foam pattern surface and investigated its effect on the surface

**Fig. 2** Slurry mixer

Fig. 3 Microstructural image of **a** Zircon sand primary coat stucco, **b** Molochite 30/60 secondary coat stucco and **c** Molochite 16/30 secondary coat stucco



(a) (b)



(c)



(d)

Fig. 4 Ceramic test samples for measuring **a** fracturability, **b** permeability, **c** porosity and **d** flexural strength

irregularity of the foam pattern, shell as well as casting. The results indicated that the wax smoothing film greatly decreased the surface roughness of ceramic shells and castings.

According to Moore and Maybaum [14], some common problems which cause rejection of the IC ceramic shells are poor strength, inadequate permeability, cracking, passage restrictions and warpage of the produced shells. Kline [15] found that most of the IC ceramic shells use to crack at edges and sharp turnings. Shaw and Duffey [16] substituted insoluble smooth-surfaced organic fibres into the ceramic slurries and they found that the fibre containing ceramic shell possessed essential shell characteristics such as adequate shell thickness (at both regular section and edges and sharp turnings), fired strength and permeability. However, the green strength of the fibre-modified shell



Fig. 5 Fracturability tester

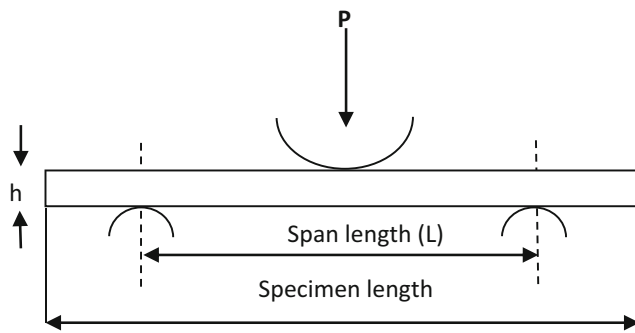


Fig. 6 Load configuration for a beam in three point bending

was found to be comparatively less due to the slippery nature of the organic fibres.

Later, it was found by Doles and Viers [17] that the addition of these smooth-surfaced organic fibres into the ceramic slurries could not always produce a replica of small holes, channels and other fine details to a great extent. Moreover, these soluble organic polymers and insoluble organic fibres are costly, which eventually amplifies the overall cost of production of the IC ceramic shells. Yuan et al. [18] investigated about the effect of increased polymer content and different firing temperatures of yttria moulds for casting titanium aluminide alloys. The results revealed that increased polymer content from 0 to 30% did not affect the mould strength prior to and after sintering. However, firing temperatures between 1200 and 1400 °C significantly augmented the strength of the shell. Yahaya et al. [19] studied the influence of activated charcoal on the physical and mechanical characteristics of ceramic shells obtained via microwave dewaxing. It was found that increased percentage of charcoal decreased the dewaxing time. Twenty-five percent of charcoal was found to be the optimum quantity that should be added to the coarse stucco for getting crack free shell.

The above literature survey throws light that there is a need to identify some additives for the IC ceramic shell which would provide adequate mechanical properties and thickness with more permeable structure at relatively less cost. In the IC process, among naturally available additives, rice husk had

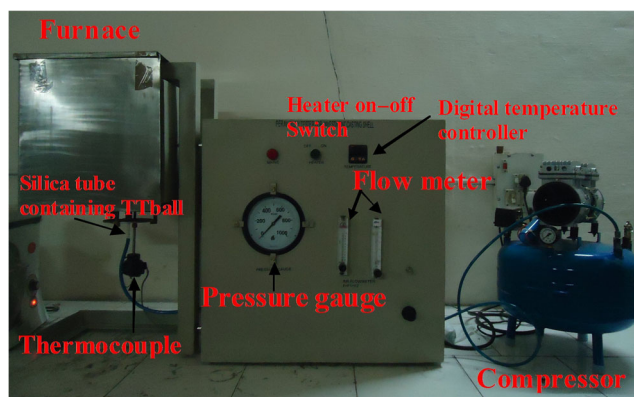


Fig. 7 Hot permeability tester

been added previously into the ceramic slurry to increase the shell's green strength [20]. Natural fibres are easily and cheaply available all over the world. Sawdust is one of the most commonly used natural fibres, which is produced by sawing off wood. Its physical properties include low density, high porosity, high water retention, low cost and resistance to breakage.

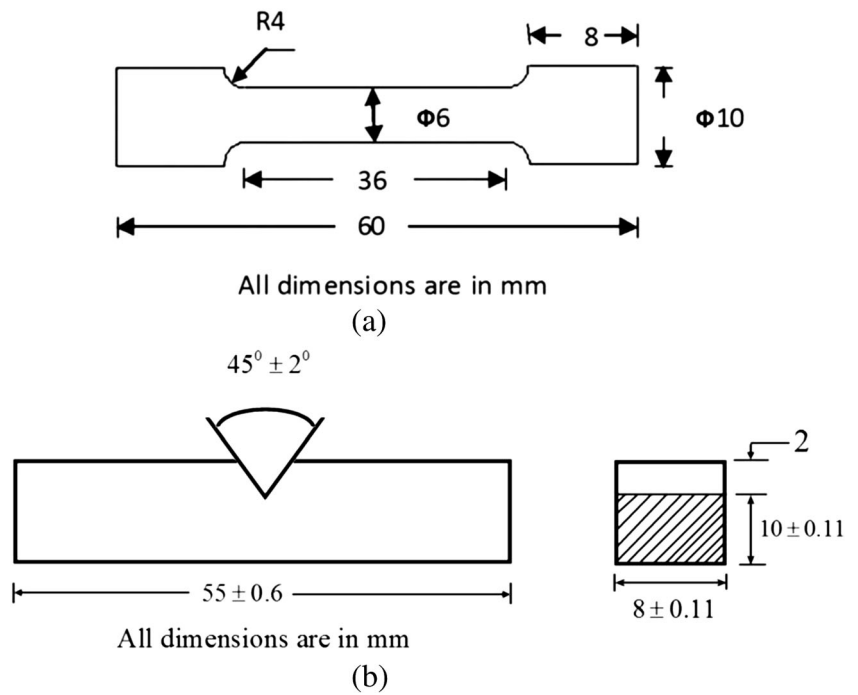
Youmou et al. [21] designed the ceramic filters using clay and sawdust mixture and investigated their mechanical, microstructural, morphological and pore network properties. It was found that mechanical properties of ceramic filter candles depended on matrix composition, firing temperature, mineral phase contained in the sample after firing and on the presence of capillary pores in fired ceramics. Sales et al. [22] studied the mechanical properties of a bio-composite made from water treatment sludge and sawdust. The produced concrete with the aforementioned composite showed sufficient mechanical strength and found suitable for non-structural constructive applications. Islam and Islam [23] prepared chemically treated sawdust-reinforced recycled polyethylene composite, and they found that the resultant composite exhibited improved mechanical properties. Duan et al. [24] verified the viability of using sawdust particles in making reinforced composites. It was found that the sawdust addition influenced the workability of the geopolymer and created most advantageous microstructure in it.

Fibre-reinforced ceramic shell is a ceramic matrix composite where fibres are the reinforcement and the main source of strength, while the matrix joins all the fibres together and shift stresses between the reinforcing fibres. However, sawdust as natural fibre has never been used as reinforcement for constructing the IC ceramic shell to enhance its properties. In the present investigation, finely sieved sawdust has been added into the secondary ceramic slurries and its influence on important shell properties such as fracturability, flexural strength, porosity and permeability have been studied. The aforesaid properties were then compared with those obtained from the conventional ceramic shell. Further, the mechanical properties, namely tensile strength and impact strength of the investment cast parts obtained from both conventional and sawdust-modified ceramic shells, were determined.

2 Experimental work

The ingredients used to prepare both conventional and sawdust-modified ceramic shells are shown in Table 1. The flow chart for building the ceramic shell around the disposable pattern is shown in Fig. 1. The refractory flour and binder were combined in a 3:1 weight ratio for the primary slurry and 2:1 weight ratio for the secondary slurry. The amount of liquid polymer, antifoam and wetting agent added was 5, 0.3 and 0.3% of weight of the slurry. The mixing of primary slurry

Fig. 8 a Cylindrical tensile specimen. b Impact specimen



and secondary slurry continued for 72 and 48 h by means of a slurry mixer, as shown in Fig. 2. When the mixture became excessively thick, distilled water was added accordingly to adjust its viscosity. Mostly, it happens that the slurry is unable to stick to the wax surface due to oil and dirt present on it, which ultimately causes casting cracking and run-outs. Thus, the constructed wax patterns were first cleaned by acetone to provide a means of slurry adhesion just before dipping in the primary slurry for 30 s. It also increases the wetting between the slurry and wax pattern surface. Then, the pattern is drained for 60 s to drain the excess slurry and sprinkled with zircon stucco of size –200 mesh by the rainfall sanding method. The shell with the first layer is dried for 24 h.

Afterwards, secondary slurry is prepared from aluminium-silicate flour of –200 mesh size and colloidal silica binder. In one case, 5 wt% liquid polymer is added and in another case, same weight percent of sawdust particles are added to the secondary slurry. Again, the process of dipping, draining, stuccoing and drying continued further three times over the previously formed layer of the wax pattern. Finally, a sealing layer of secondary layer without stucco is formed and dried for 24 h. The shells with the wax pattern are then placed in a microwave oven for about 15 min for dewaxing. The green

shells thus obtained are fired at high temperatures inside a top open muffle furnace. Now, the shells are ready for casting.

The stucco size gradually increases as shown in Fig. 3. It is clearly visualized that the zircon sand used as stucco for the primary layer is the finest and Molochite 16/30 (secondary layer stucco) is the roughest. In backup layers, increased stucco size results in larger pore size of the shell. However, these coarse stucco particles help in seizing the further drainage of the slurry, supports good bonding between individual layers and shell thickness is quickly achieved. The physical properties of the sawdust which influence the properties of the ceramic shell are its density, porosity and particle size. Ceramic test samples were prepared for measuring fracturability, flexural strength, porosity and

Table 2 Physical properties of additives used in the ceramic slurry

Physical properties	Sawdust	Liquid polymer
Density (g/cm ³) ASTM C134	0.22	1.05
Apparent porosity (%) ASTM C20	76	40
Particle size (µm) SEM image	170–320	–

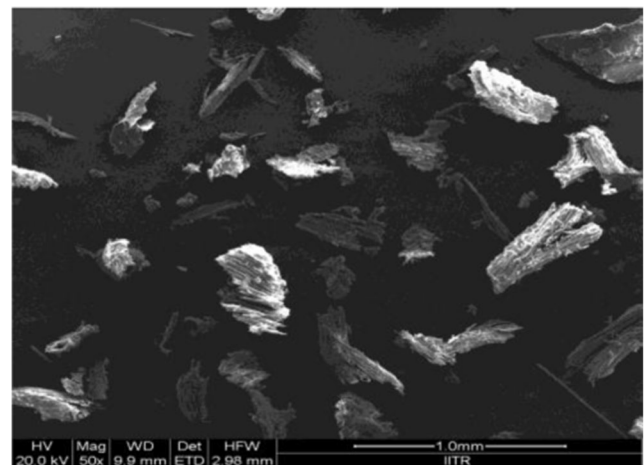


Fig. 9 Microstructure of sawdust particles at low magnification

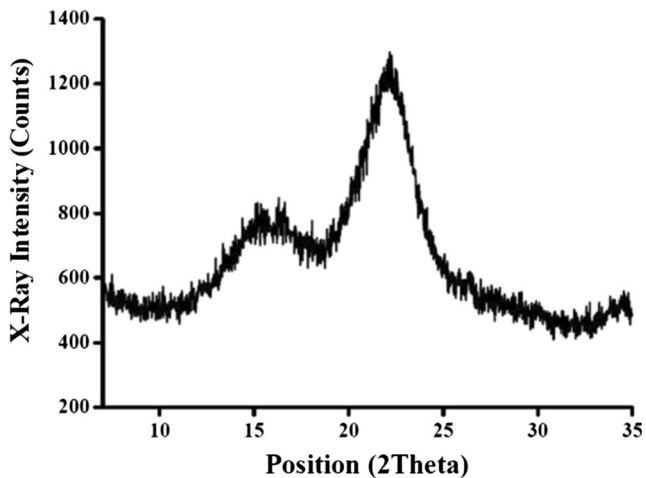
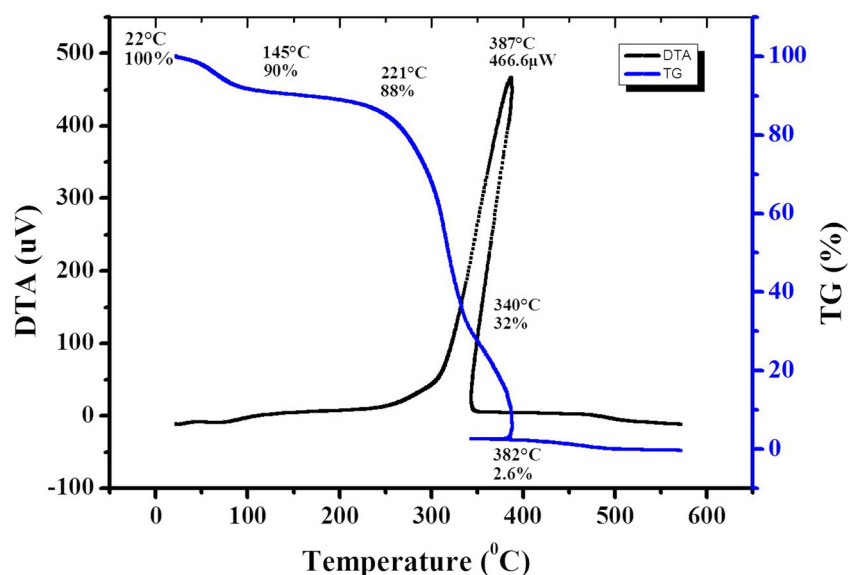


Fig. 10 XRD spectrum of sawdust

permeability of the shells using the wax blend investigated by Pattnaik et al. [25].

The addition of sawdust in the secondary slurry was restricted to 5 wt.% as the accumulation of sawdust beyond this limit decreased the fired strength of the shell which led to the generation of small cracks around the ceramic shell during the shell drying stage. Also, slight black coring was observed in the primary layer (in some cases) after the shell firing stage. The important slurry parameters such as viscosity, pH, density and plate weight of the slurry were measured in both cases. The slurry viscosity and pH were measured using a Brookfield Viscometer and pH meter. Density was measured by the conventional mass and volume method. Plate weight or slurry retention rate was measured as per Sidhu et al. [26]. The ceramic samples constructed for measuring properties, namely fracturability, flexural strength, porosity and permeability are shown in Fig. 4.

Fig. 11 DTA and TG curves of sawdust



The objective to study the fracturability of the primary layer of the ceramic shell is to evaluate the extent of fracture of the filler particles during shell firing. When the shell is filled with the molten alloy, there are chances that these fractured filler particles may enter into the melt and contaminate the casting. In order to measure the fracturability of the sample, the diameter (d) and height (h) of the hollow cylindrical ceramic shell were measured. The initial weight (W_i) of the ceramic shell was recorded. Then, a nylon brush was pushed inside the ceramic shell fully and rotated so that the teeth of the brush touch the inner wall of the shell as shown in Fig. 5. Later, the brush was pulled out and the shell was reweighed (W_b). The formula for fracturability (F_t) in gramme/square centimetre of the ceramic sample is given by Eq. 1. Low fracturability value is advantageous as it would show less wearing away of the inner coat of the shell.

$$F_t = \frac{W_i - W_b}{\left(\pi dh + \frac{\pi d^2}{4}\right)} \quad (1)$$

Flexural strength or modulus of rupture (MOR) testing of the ceramic shells was done using a computerized UTM of the make Tinius Olsen with a capacity of 2.5 kN. The specimen dimensions were made as per ASTM D7264M [27]. For each type of shells, three specimens were prepared and tested. The bending load was given a velocity of 1 mm/min. In three-point bending, the load configuration is shown in Fig. 6. The flexural strength (MPa) is calculated using the following equation:

$$\sigma_m = \frac{3PL}{2bh^2} \quad (2)$$

Table 3 Characteristics of slurry properties for conventional and sawdust-modified shells

Properties	Unit	Primary slurry	Conventional polymer-modified secondary slurry	Sawdust-modified secondary slurry
Density	gm/cm ³	3.049	1.423	1.579
Viscosity	cp	1840	1132	1228
pH	–	9.5	9.4	9.4
Plate weight	g/cm ²	0.179	0.112	0.125

where P is the fracture load (N), L is the span length (mm), b is the width of the test-piece (mm) and h is its height (mm).

The apparent porosity of the ceramic specimens (% AP_{Shell}) was measured using Eq. 3 as per ASTM C20, given by Berger [28].

$$\%AP_{Shell} = \frac{(W_W - W_D)}{(W_W - W_S)} \times 100 \tag{3}$$

where W_W , W_D and W_S are soaked, dry and suspended weights of ceramic shell, respectively.

The hot permeability (k) of the ceramic shell was measured at 900 °C using a permeability tester as shown in Fig. 7 as per Amira et al. [29]. The compressed air was made to gush into the heated ceramic shell. The air flow rate (F) was changed by means of flow meters, and the resultant pressure drops ($\Delta P = P_i - P_o$) were determined via pressure gauge.

The knockability is the ease with which the cast part is removed from the shell mould. The knockout operation of the shell is done by various means such as by using mechanical vibrators, sand blasting or mechanically breaking the shell. As the cast part is solidified, little fired strength of the shell is yearned to assist the knockout action [30]. There is no standard procedure to measure the knockability of the shell.

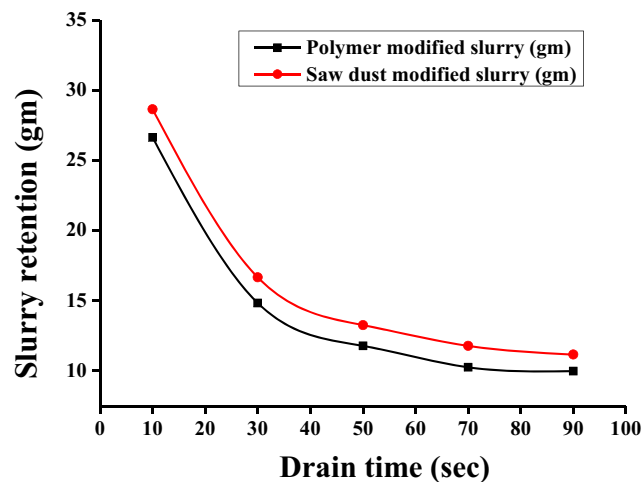


Fig. 12 Graph showing drain time versus retention of polymer and sawdust-modified slurry

The author had broken the shell by means of little hammering the shell manually. On the basis of ease at which the fragile shell ruptured, it was estimated whether the knockability of the shell is good or bad.

The mechanical properties namely tensile strength and impact strength of the hypoeutectic Al-Si alloy castings obtained from both shells were measured as per ASTM standards E8/E8M [31] and E23 [32]. The sample dimensions for testing both tensile and impact strengths are shown in Fig. 8. The Charpy method with a V-notched angle of 45° was used to study the impact toughness.

The crystalline structure of the sawdust and the primary layer of the ceramic shell was measured by X-ray diffractometer (D8 Advance, Bruker AXS, Karlsruhe, Germany) within a 2θ range from 10 to 90° in Cu-K α radiation through a Ni filter at a tube current of about 20 μ A and a voltage of 35 Kv.

3 Results

3.1 Physical properties of sawdust

The physical properties of sawdust and liquid polymer are shown in Table 2. The density of sawdust was found to be very less, i.e. 0.22 g/cm³, and its apparent porosity was found to be very high, i.e. 76%, as compared to that of the conventional liquid polymer. This low density of sawdust makes it highly porous. The surface morphology of sawdust is shown in Fig. 9, and it is seen that the sawdust particles are irregular in shape and coarse in appearance. This was the rationale behind not adding them to the primary slurry as primary layer

Table 4 Comparison of shell thickness

Type of ceramic shell	Mean thickness at regular section (mm)	Mean thickness at sharp corner (mm)
Conventional	4.74	3.45
Sawdust-modified	5.51	4.76
Improvement of thickness of sawdust-modified shell over conventional shell (%)	16	38

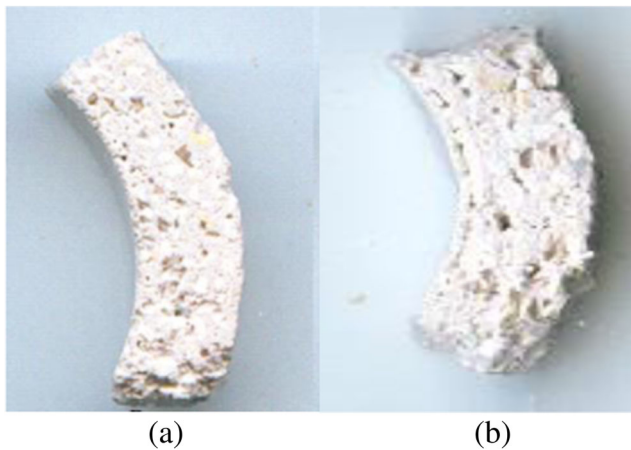


Fig. 13 Images of thickness at regular section for **a** conventional shell and **b** sawdust-modified shell

is always in direct contact with the wax pattern. The average grain size of sawdust was found to be in between 170 and 320 μm . The XRD spectrum of sawdust is shown in Fig. 10 and the peaks are found at 2θ of 16 and 22.2° , which is the characteristic spectrum of cellulose. This cellulose includes a series of glucose rings, which leads to important structural and mechanical characteristics in the fibre itself [33].

Thermo gravimetric (TG) and differential thermal analysis (DTA) curves of sawdust are shown in Fig. 11. The TG curve shows the overall loss in mass of sawdust occurs at three different stages, mainly during removal of adsorbed moisture and disintegration of both cellulose and lignin. By heating sawdust from 22 to 145°C , mass loss was found to be 10%, owing to the elimination of moisture from it. On further heating from 145 to 221°C , mass loss was only 2%. When the temperature was raised from 221 to 340°C , the mass loss was 56%, which was due to the decomposition of cellulose. The lignin was decomposed in the temperature range from 340 to 382°C , whose mass loss was 29.4%. Thereafter, on increasing temperature beyond 382°C , there was no further loss in mass of sawdust. Thus, it is apparent from the TG analysis that the cellulosic content of sawdust undergoes higher decomposition than its lignin content. From the DTA curve, the burning temperature of sawdust was found to be

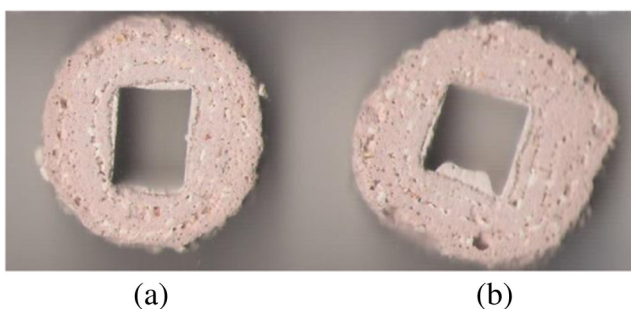


Fig. 14 Images of thickness at sharp corner for **a** conventional shell and **b** sawdust-modified shell

387°C , which is almost coinciding with its final decomposition temperature.

3.2 Slurry characteristics and shell thickness

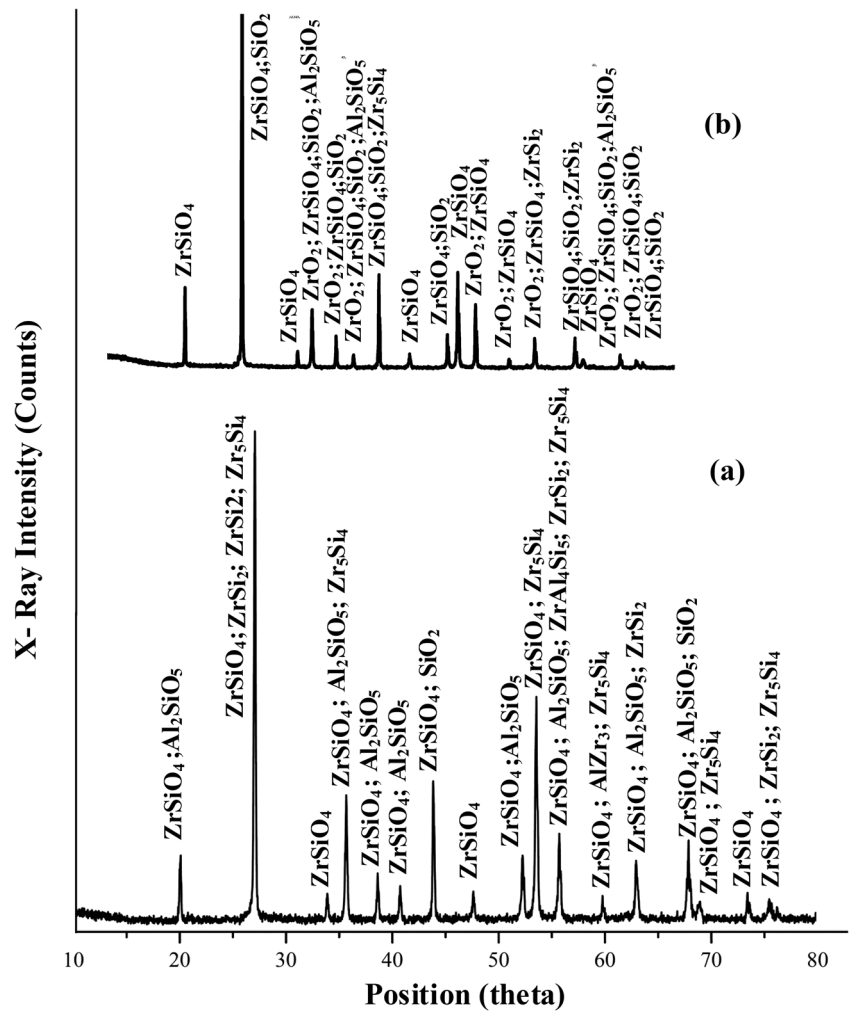
In Table 3, the slurry characteristics for different coats for both kinds of ceramic shells have been shown. It is clearly seen that the primary coat exhibited increased slurry rheological properties as regards to secondary slurries. It is favourable as primary slurry forms the ceramic face of the shell mould. Water-based primary slurry requires the use of deionized water for good control of slurry properties. The secondary coatings serve different functions from that of the primary layer and thus, materials used to construct the secondary layers are different from those of the primary layer, which causes different slurry characteristics. It is seen that the sawdust-modified ceramic slurry possessed 11% higher density, 8.5% more viscosity and 11.6% extra plate weight than that of the conventional polymer-modified secondary ceramic slurry which is due to the higher ceramic retention rate and reduced drain time of the former over its counterpart as apparent from Fig. 12.

The thickness of both conventional and sawdust-modified shells at regular section and sharp corner are shown in Table 4, and the corresponding images are depicted in Figs. 13 and 14, respectively. It is seen that the thicknesses of the sawdust-modified shell are greater by 16% at regular section and 38% at sharp corner as compared to that of the conventional ceramic shell for a five-layered shell system. It is due to the fact that the fibrous sawdust particles increased the coagulation efficiency of the slurry which increased its viscosity and ceramic retention rate. Thus, it can be said that an equivalent mould thickness could be achieved with reduced number of secondary coats using sawdust-modified slurry.

3.3 Fracturability

The fracturability values of both conventional and sawdust-modified ceramic shells were found to be 0.002598 and 0.002617 g/cm^2 , respectively. The lesser the fracturability of the shell, the smaller is the chances of inclusions in the casting. Thus, the lowest value of fracturability is desirable for all the ceramic shells. It is clear that the fracturability of the conventional shell is lesser than the sawdust-modified shell. But, both values are nearby equal and the difference might have aroused due to the measurement error. As the fracturability test was done on the primary layer of both shells, it is obvious that both of them would show almost similar fracturability characteristics owing to similar primary layer composition and the firing temperature. However, this test was done to check the infiltration of stucco or sawdust particles into the primary layer thereby eroding it. Thus, it shows that the fracturability of the primary layer of the ceramic shells is not influenced by the addition of additives in the secondary layers.

Fig. 15 XRD analysis of primary layer of ceramic shell. **a** Conventional. **b** Sawdust-modified



Later, XRD analysis of the primary layer of both shells was done to verify it additionally. The XRD phase diagrams of both shells after casting the Al-Si alloy are depicted in Fig. 15. The various phases present in both shells were found to be ZrSiO₄, ZrO₂, SiO₂, Al₂SiO₅ and ZrSi₂ [26]. However, it is clear that both spectra have resemblance with each other and the prominent phases are ZrSiO₄ and SiO₂ (ZrSiO₄ from the zircon floor and SiO₂ from the colloidal silica binder). It shows that the composition of the secondary layer of both shells did not affect the composition of the primary layer.

Table 5 MOR results of both conventional and sawdust-modified shells

Sl. no.	Conventional shell		Sawdust-modified shell	
	Green (MPa)	Fired (MPa)	Green (MPa)	Fired (MPa)
1	2.232	1.986	2.503	1.603
2	2.461	2.115	2.637	1.64
3	1.957	1.742	2.617	1.58
Mean	2.217 ± 0.252	1.948 ± 0.189	2.586 ± 0.072	1.608 ± 0.03

The primary layer of both shell types (polymer-modified and sawdust modified) were made from the same slurry. So, it was expected that the phases should be the same. However, there are chances that during shell firing and aluminium alloy casting, impurities from the shell and cast metal may come in contact with the primary layer. For superior control of water-based primary slurry properties, close attention to the raw material impurities should be given. From the figure, it can be seen there is no significant amorphous peak. A slight variation may occur due to experimental conditions, handling differences, environmental conditions and intrinsic ceramic variability.

3.4 Flexural strength

MOR is nothing but a fracture stress and the fracture load and specimen dimensions influences it. Shell thickness is particularly very important, as the stress is inversely proportional to its squared value [34]. An IC ceramic shell usually possess a course surface, and this rough surface of ceramic shell causes difficulty in accurately measuring the shell dimensions, which

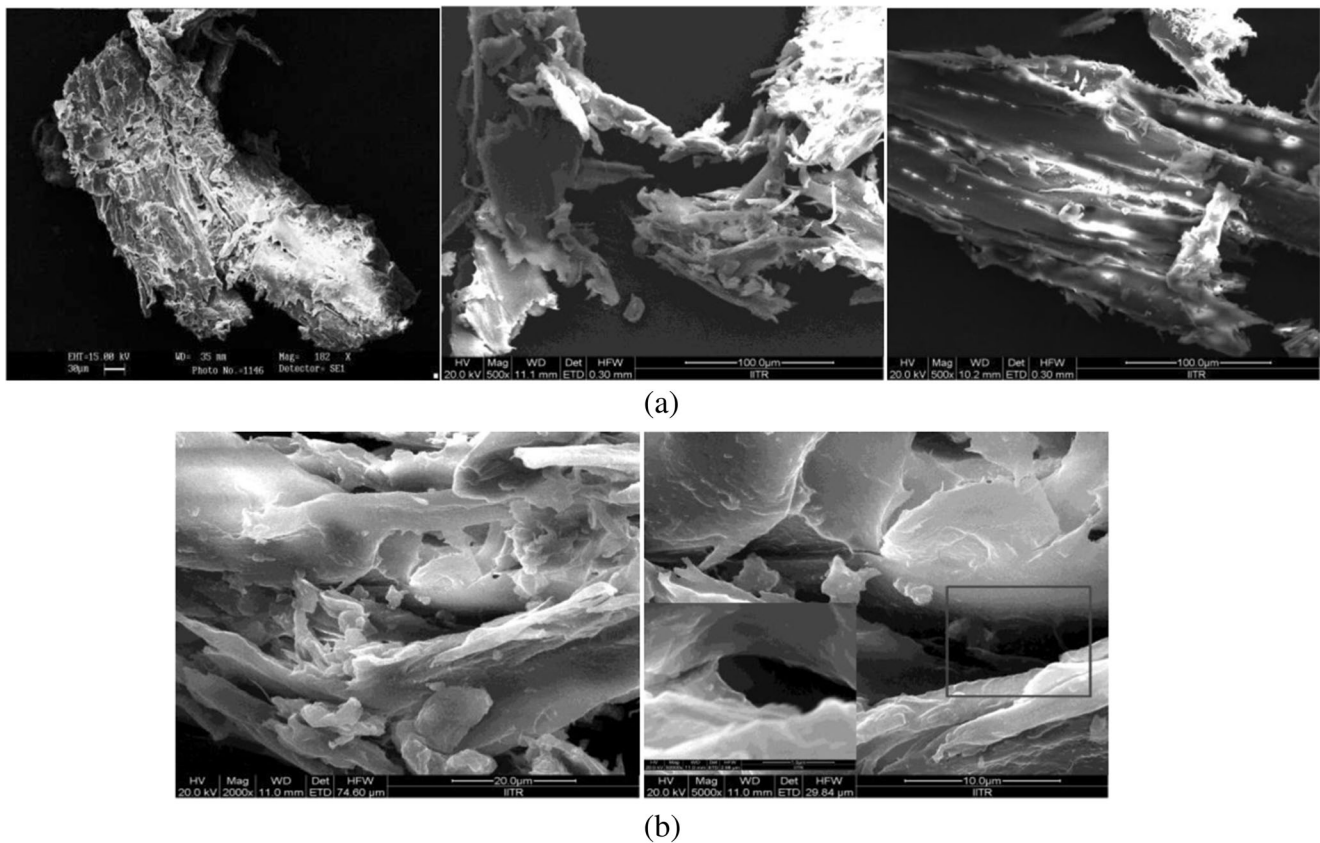


Fig. 16 Microstructure of sawdust particle at **a** low magnification and **b** high magnification

results in large standard deviations. This insufficiency is defeated by testing a sufficient number (at least three) of test specimens. The flexural strength or MOR of both conventional and sawdust-modified ceramic shells at green and fired states was measured, and the results are shown in Table 5. It is evident that the sawdust-modified ceramic shell showed higher green strength and lesser fired strength as compared to that of the conventional ceramic shell. This could be better explained from the SEM micrographs of sawdust and sawdust-modified shell.

The SEM image of sawdust is shown in Fig. 16a [31] and it is apparent that its surface is very fibrous. At higher magnification (Fig. 16b), it is observed that this fibrous surface contains many irregular scales. These scales are attached to one another in such a way that a small trough is formed at irregular spaces. The SEM image of green ceramic shell containing sawdust is shown in Fig. 17. It is seen from Fig. 17a that sawdust has been completely united with the ceramic slurry and formed an efficient interfacial adhesive bond between itself and the ceramic matrix thereby increasing the shell's green strength. The bonding between the coarse sawdust particles and the ceramic material was so strong that it was very difficult to remove them by pulling action. Further, the density of sawdust (0.22 kg/cm^3) was less than the density of the liquid polymer (1.02 kg/cm^3) and thus, more amounts of sawdust particles were embedded in the slurry for

equal wt% of liquid polymer. Consequently, the packing of sawdust particles within the ceramic matrix was comparatively more than the liquid polymer.

Even though the ceramic shell was dewaxed in oven, sawdust embedded within the ceramic matrix remained integral. These

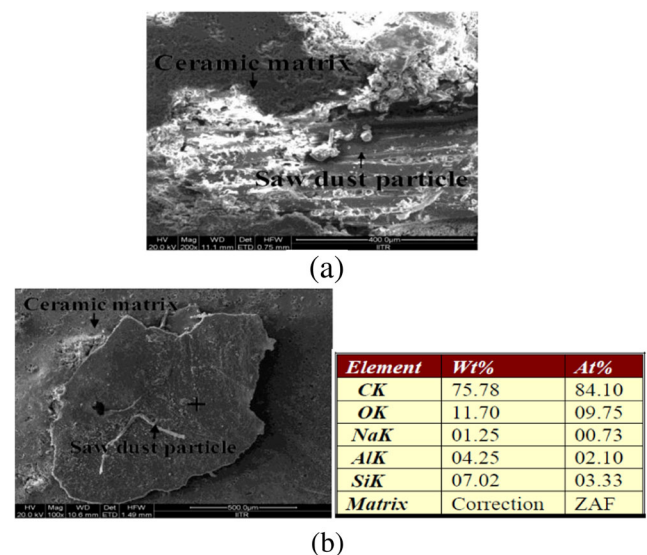


Fig. 17 Microstructures of **a** sawdust particle in ceramic matrix and **b** top view of the embedded sawdust particle in ceramic matrix

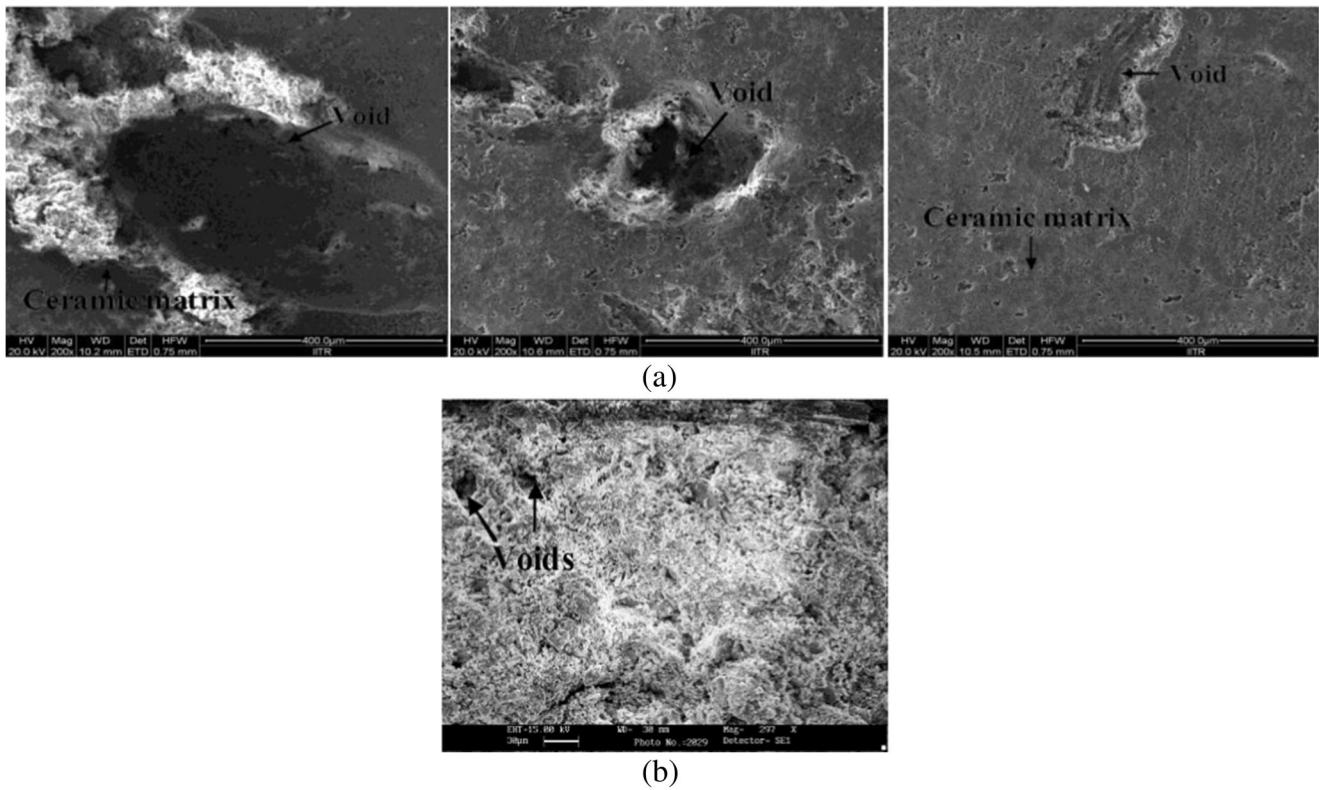


Fig. 18 SEM image showing voids created by burn out of **a** sawdust and **b** liquid polymer

were not burnt because the burning temperature of sawdust was higher than the shell’s dewaxing temperature as evident from the DTA curve of sawdust. The SEM image of the top view of the embedded sawdust particle in the ceramic matrix followed by its compositional analysis is shown in Fig. 17b, which illustrates that it mostly contains carbon. Other elements include sodium, aluminium and silicon due to the composition of the secondary slurry.

The SEM micrographs of both fired sawdust-modified and conventional polymer-modified ceramic shells are depicted in Fig. 18. The voids created due to the burn out of both particles in the ceramic matrix on shell firing are clearly visible. However, it is apparent that the voids created owing to the burn out of sawdust are much bigger than that created by its counterpart.

Due to more number of large-sized pores, the sawdust-modified shell showed lesser fired strength as compared to that of the conventional polymer-modified ceramic shell. It is further expected that the porosity of the aforementioned shell would be higher than its counterpart.

3.5 Porosity and permeability

The measured value of apparent porosity for both conventional and sawdust-modified ceramic samples at fired state is furnished in Tables 6 and 7, respectively. The lower and upper boundaries of % AP_{Shell} determined for conventional ceramic shells are approximately 16 and 17%, whereas the same for sawdust-modified ceramic shells are approximately 27 and

Table 6 % AP_{Shell} of fired conventional polymer-modified ceramic shell

Sl. no.	W_D (gms)	W_W (gms)	W_S (gms)	$W_W - W_D$ (gms)	$W_W - W_S$ (gms)	$\%AP_{Shell} = \frac{(W_W - W_D)}{(W_W - W_S)} \times 100$
1	98.930	106.501	60	7.571	46.501	16.281
2	98.976	106.802	60	7.826	46.802	16.722
3	97.882	105.465	61	7.583	44.465	17.053
4	98.865	106.824	60	7.959	46.824	16.998
5	98.647	105.980	62	7.333	43.980	16.673

W_W , W_D and W_S are soaked, dry and suspended weights of ceramic shell, respectively

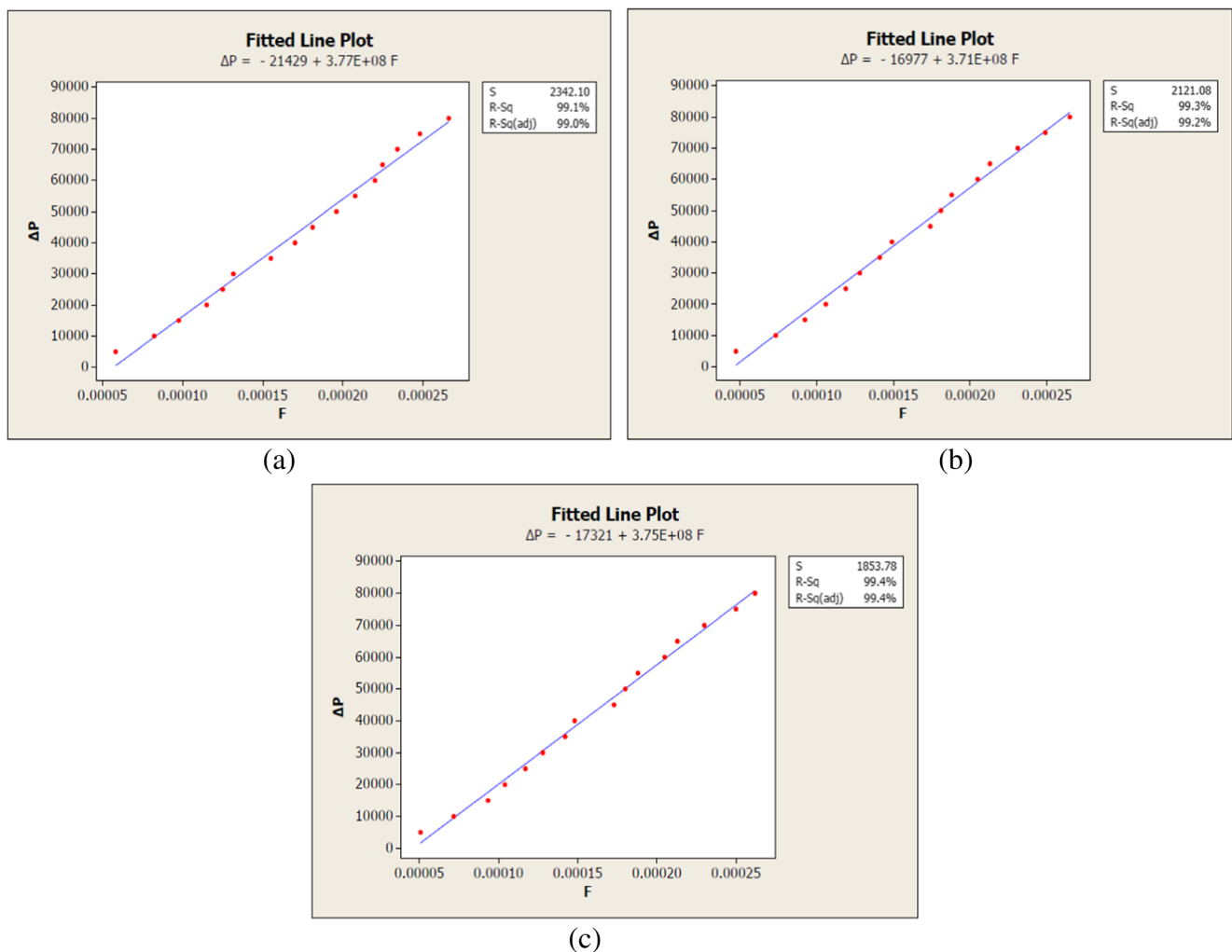
Table 7 % AP_{Shell} of fired sawdust-modified ceramic shell

Sl. no.	W_D (gms)	W_W (gms)	W_S (gms)	$W_W - W_D$ (gms)	$W_W - W_S$ (gms)	$\%AP_{Shell} = \frac{(W_W - W_D)}{(W_W - W_S)} \times 100$
1	96.984	112.063	58	15.079	54.063	27.892
2	98.823	115.791	60	16.968	55.791	30.413
3	98.671	114.243	60	15.572	54.243	28.708
4	97.889	112.933	62	15.044	50.933	29.537
5	98.573	114.209	61	15.636	53.209	29.386

W_W , W_D and W_S are soaked, dry and suspended weights of ceramic shell, respectively

31%. The overall porosities of the conventional and sawdust-modified ceramic shells are 16.75 and 29.19%, respectively. This shows that the porosity of sawdust-modified ceramic shell is 74% higher than the conventional ceramic shell. Standard deviation is an extensively used method of measurement of variability or diversity in statistics. A low standard deviation shows that the data points are very close to the mean, whereas high

standard deviation indicates that the data are spread out over a large range of values. It is observed that the standard deviation of fired conventional polymer-modified shell is less than that of fired sawdust-modified shell, which shows that the porosity of the former shell is comparatively less affected by handling differences, slurry rheology, measurement errors, etc. as regards to the later shell type. The results obtained for the apparent porosity

**Fig. 19** a–c Regression curves of three conventional shell specimens fired at 900 °C

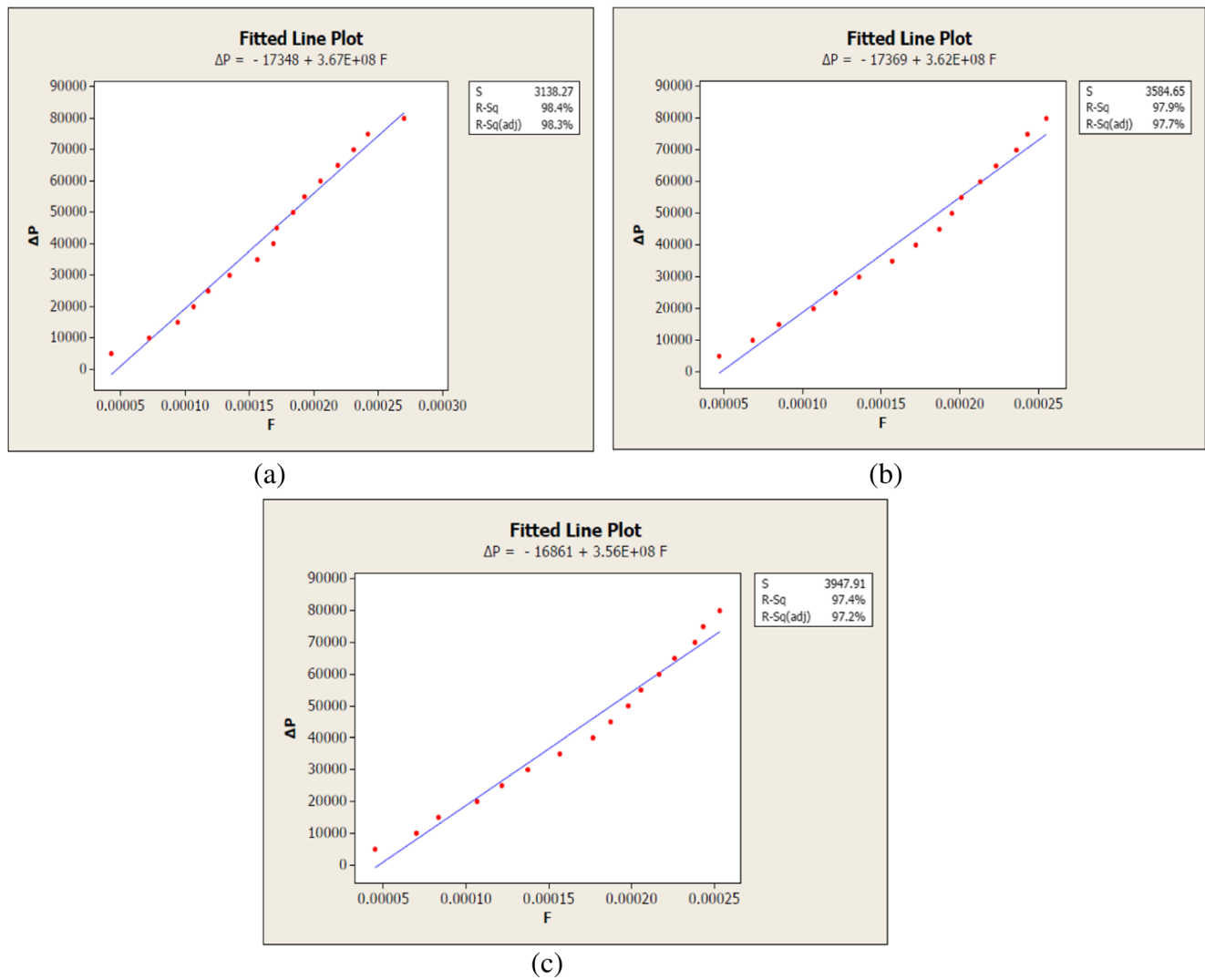


Fig. 20 a–c Regression curves of three sawdust-modified shell specimens fired at 900 °C

of both ceramic shells are very well in agreement with the inference drawn from the microstructural analysis of both shells at fired condition.

For measuring the permeability of the ceramic shells, regression curves of ΔP versus F were plotted and regression equations were determined as shown in Figs. 19 and 20. Permeability values determined for both shells are shown in Table 8, and it is apparent that the permeability of the sawdust-modified ceramic shell is 20% higher than the conventional ceramic shell.

Inadequate shell’s porosity or permeability leads to casting defects such as misrun and porosity in the cast parts. Misrun is

caused due to the inability of the molten alloy to fill the ceramic shell completely which leads to imperfect casting as shown in Fig. 21. The ceramic shell is enclosed by air and when the molten alloy is poured into the heated shell, the air should be ejected out as quickly as possible; otherwise, the back pressure of air interrupts in filling of the complete shell. Besides air, hot gases generated while heating the molten alloy are also present and if they are not expelled out of the shell speedily, they would be entrapped inside the casting causing small-sized pores inside it. The cross-sectional view of the Al-Si alloy casting obtained from the impervious shell is shown in Fig. 22. Numerous unevenly shaped pores could be clearly

Table 8 Experimental values of k for both ceramic shells

Conventional shell		Sawdust-modified shell	
Mean k ($\times 10^{-14}$) m^2	Shell thickness	Mean k ($\times 10^{-14}$) m^2	Shell thickness
7.94	4.74 mm	9.51	5.51 mm

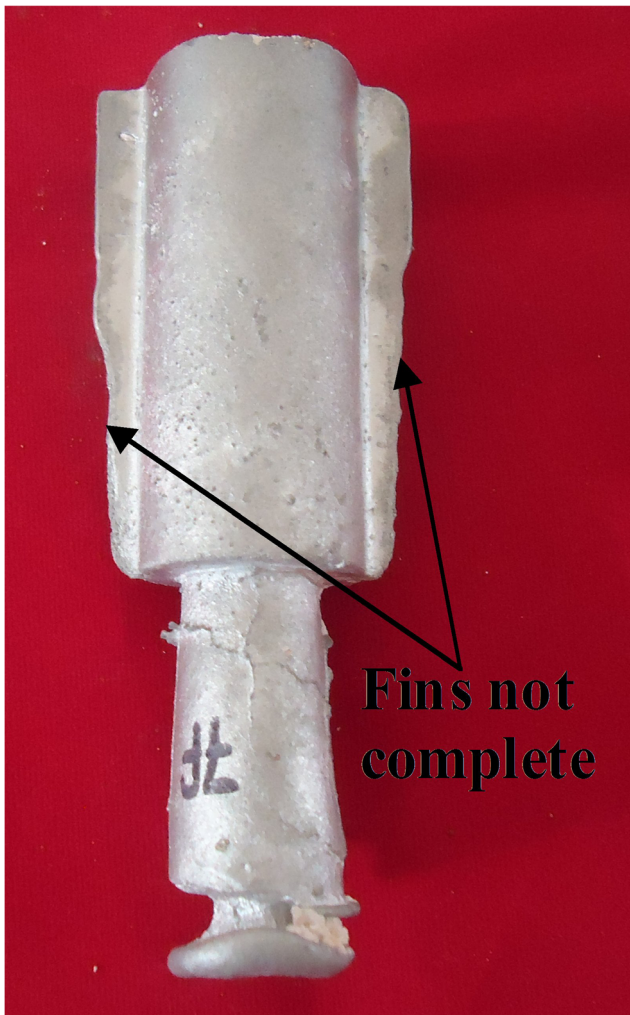


Fig. 21 An incomplete investment casting

seen, and this porosity in casting reduces the mechanical properties of the cast part which is not favourable. Thus, it is essential that the ceramic shell should be sufficiently permeable to prevent misrun and porosity defects in investment casting.

3.6 Mechanical properties of aluminium alloy castings

The results of tensile and impact strengths of the castings obtained from both conventional and sawdust-modified shells are summarized in Table 9. It is clear that the tensile strength and impact strength of the Al-Si alloy investment castings obtained from the sawdust-modified shells are comparatively higher by 6.4 and 20% than those obtained from the conventional shells.

The mechanical properties of any casting depend on alloy composition, grain size, cooling rate, extent of porosity present in it, etc. The casting cooling rate in sawdust-modified shell was found to be comparatively faster due to its more porous and permeable structure over the conventional shell,



Fig. 22 Occurrence of porosity in investment casting

and it led to fine grain structure of the Al-Si alloy investment casting and improved its mechanical properties.

4 Discussions

The binders used in the IC process are either alcohol-based or water-based. As per the type of the binder employed in building the ceramic shell mould, the shell properties have to be regulated. The ceramic shells should possess adequate thickness, green and fired strengths, porosity and permeability. The thickness of the ceramic shell influences the shell's strength. For the alcohol-based shells, thickness is not an issue as they are extremely strong (at both green and fired states) to withstand various pressures during casting. Thus, it is immaterial to increase the flexural strength and thickness of the shells prepared from alcohol-based binders. However, the porosity and permeability of these ceramic shells are extremely poor. Any miscible and flammable material may be used as a pore-former for increasing the permeability of these shells as it would get burnt and create void in its place on shell firing. The impervious nature of the ceramic shell is common to both shells whether they are made from water-based or alcohol-based binders.

Knockability is another important property of IC ceramic shell which is inversely proportional to the shell's fired strength. It was found from the pilot experiments that the knockability of the ceramic shell prepared from alcohol-based ethyl silicate binder was very poor, and there were chances of casting damage while breaking the firm shell. However, the knockability of the shells made from water-based colloidal silica binder was found to be extremely good. The main shortcoming of the colloidal silica-based shells is that they lack adequate green strength. The green strength of the ceramic shell made from colloidal silica binder can only be

Table 9 Mechanical properties of both conventional and sawdust-modified shells

Conventional shell		Sawdust-modified shell	
Mean tensile strength (MPa)	Mean impact strength (J/mm ²)	Mean tensile strength (MPa)	Mean impact strength (J/mm ²)
104.3	2.5	111	3.0

increased if the additive forms a strong adhesive bond with the ceramic matrix. The fibrous structure of additive is a boon to strengthen this bond. It should be noted that the additive should not get burnt while dewaxing. Otherwise, the linkage between itself and the ceramic matrix would be poor.

Fibre is a small reinforcing material possessing certain characteristics. They may be circular or flat. The natural fibres exhibit discrepancy in properties such as chemical composition, crystallinity, diameter, length, cross-sectional shape, surface properties, strength and stiffness [35]. Therefore, sawdust particles have a different shape and size as compared to other natural fibres such as coir. However, its fibrous surface is clearly visible in microstructural images which causes a good bonding between the ceramic matrix and the sawdust so that the stress is transferred from the ceramic matrix to the embedded sawdust in the shell. The quantity of sawdust affects the strength of the shell. As sawdust particle is very light in weight, more amounts of sawdust particles as compared to liquid polymer were added to the slurry. The sawdust addition into the ceramic slurry has brought potential improvement in the shell's green strength (excess strength is undesirable as it creates difficulty in shell collapsibility to safely take out the cast part). It was found from the trial experiments that the percent increase in amount of sawdust up to 5 wt% increased the green strength of the shell. However, beyond that, the fired strength decreased causing shell cracking though shell permeability increased. Sawdust used in this study was chosen on the basis of its burning temperature (DTA curve) which remained intact with the ceramic matrix after dewaxing, as evident from the SEM images.

Besides green strength, a ceramic shell must also have sufficient fired strength so as to bear the weight of the hot melt during casting. If its fired strength exceeds than that required, the knockout operation of the shell to remove the casting becomes very difficult. Most of the IC shells contain ample amounts of silica, and when these shells are heated at temperatures above 1000 °C during casting of ferrous or super alloys, amorphous silica crystallizes and forms beta-cristobalite. Later, beta-cristobalite is converted into its alpha form. This phase change causes alteration in the shell's volume. Consequently, many cracks are generated in the shell which assists in easy shell removal. The existence of the cristobalite phase is crucial for effortless knockout operation of the shell. However, cristobalite could not be formed in the silica containing IC shells while casting non-ferrous alloys, since their melting and pouring temperatures are less than 1000 °C. Still,

their fired strength was reduced in this study as the internal structure of fired sawdust-modified shell was found to be very porous and permeable.

Further, the results obtained from the present research have been superficially compared with that obtained from Kline et al. [15]. The researchers had added graphite particles in the ceramic shell to increase the shell's permeability, though the composition of the shells prepared by them was different from that of the current research work. The thickness of the graphite particle-modified shell was found to be about 4.07 mm, whereas the same for sawdust-modified shell was found to be 4.76 mm. The apparent porosities of the fired graphite particle-modified and sawdust-modified ceramic shells were found to be 26 and 29.19%, respectively. However, the flexural strength of the graphite particle-modified shell was found to be higher than that of sawdust-modified ceramic shell. But, the flexural strength of the sawdust-modified shell was sufficient to cast the alloy successfully. Further, sawdust are more cheaply and easily available as compared to graphite particles. It was found from the present study that the sawdust-modified shell showed better results from that of conventional polymer-modified ceramic shells. The mechanical properties of the casting were also higher than those obtained from conventional shells. Future work will focus on performing sawdust surface treatments so as to get comparatively more rough surface, and when it will be inserted into the ceramic slurries, it may further increase the binding strength between the fibre and the ceramic matrix.

5 Conclusions

The following conclusions are drawn from the present study:

- The thickness of the sawdust-modified shell was higher by 16% at regular section and 38% at sharp corner from that of the conventional ceramic shell for a five-layered shell system.
- The fracturability of the primary layer of both ceramic shells exhibited similar results and their XRD spectra also showed identical phases.
- The sawdust-modified ceramic shell exhibited higher green strength and lesser fired strength as compared to that of the polymer-modified ceramic shell.

- The apparent porosity and permeability of the sawdust-modified ceramic shell were 74 and 20% more than the conventional ceramic shell.
- The tensile strength and impact strength of the Al-Si alloy investment castings obtained from the sawdust-modified shells were comparatively higher by 6.4 and 20% than those obtained from the conventional shells.
- The above analysis shows that sawdust addition enhanced the shell quality at relatively less cost and time, as only few coats of the modified slurry provided the necessary thickness and strength (both green and fired) required for handling dewaxing pressure as well as melt pouring load on the shell. On shell firing at high temperatures, the additives got burnt and micro-pores are created at appropriate positions causing reduction in fired strength and enhancement of shell porosity. Thus, it is recommended for commercial application in the IC process which will ultimately reduce the cost as well as lead time of constructing the qualitative ceramic shell.

References

1. Beeley PR, Smart RF (1995) Investment casting, first edn. The Institute of Materials, London
2. Pattnaik SR, Karunakar DB, Jha PK (2012) Developments in investment casting process—a review. *J Mater Process Tech* 212: 2332–2348
3. Kalpakjian S, Schmid S (2008). Manufacturing processes for engineering materials, fifth ed. Pearson Education Incorporation
4. Pattnaik SR, Karunakar DB, Jha PK (2014) (2014). Utility-fuzzy-Taguchi based hybrid approach in investment casting process. *Int J Interact Des Manuf* 8:77–89
5. Pattnaik SR, Karunakar DB, Jha PK (2013) Parametric optimization of the investment casting process using utility concept and Taguchi method. *P I Mech Eng L- J Mater Design Appl* DOI. doi:10.1177/1464420713487654
6. Pattnaik SR, Karunakar DB, Jha PK (2013) Modeling and parametric optimization of investment casting process by uniting desirability function approach and fuzzy logic. *Journal of Intelligent and Fuzzy Systems - IOS Press*. doi:10.3233/IFS-130809
7. Pattnaik SR, Karunakar DB, Jha PK (2013) Multi-characteristic optimization of wax patterns in the investment casting process using grey-fuzzy logic. *Int J Adv Manuf Technol* 67:1577–1587
8. Bonilla W, Masood SH, Iovenitti P (2001) An investigation of wax patterns for accuracy improvement in investment cast parts. *Int J Adv Manuf Technol* 18:348–356
9. Wang D, He B, Liu S, Liu C, Fei L (2015) Dimensional shrinkage prediction based on displacement field in investment casting. *Int J Adv Manuf Technol*. doi:10.1007/s00170-015-7836-1
10. Guerra M, Schiefelbein GW (1994) Review of shell components, shell characteristics and properties: refractory selection for primary shell coat. In: Proceedings of the Investment Casting Institute 42nd Annual Meeting, Atlanta, pp. 25–28
11. Ertuan Z, Fantao K, Yanfei C, Ruirun C, Yuyong C (2012) Characterization of zirconia-based slurries with different binders for titanium investment casting. *Research & Development* 9(2): 125–130
12. Jafari H, Idris MH, Ourdjini A, Kadir MRA (2013) An investigation on interfacial reaction between in-situ melted AZ91D magnesium alloy and ceramic shell mold during investment casting process. *Mater Chem Phys* 138:672–681
13. Liao D, Fan Z, Jiang W, Shen E, Liu D (2011) Study on the surface roughness of ceramic shells and castings in the ceramic shell casting process based on expandable pattern. *J Mater Process Tech* 211: 1465–1470
14. Moore JR, Maybaum S (1986) Processes for the application of refractory compositions to surfaces such as for the preparation of refractory shell molds and refractory compositions produced thereby. US Patent No. 4624898 A
15. Kline DM (2010) Controlling strength and permeability of silica investment casting molds. Missouri University of Science and Technology, Thesis
16. Shaw RD, Duffey DJ (2004) Investment casting, US Patent No. 6769475 B2
17. Doles RS, Viers DS (2009) Filler component for investment casting slurries. US Patent No. 7588633 B2 (September 15)
18. Yuan C, Compton D, Cheng X, Green N, Withey P (2012) The influence of polymer content and sintering temperature on yttria face-coat moulds for TiAl casting. *J Eur Ceram Soc* 32:4041–4049
19. Yahaya B, Izman S, Idris MH, Dambatta MS (2016) Effect of activated charcoal on physical and mechanical properties of microwave dewaxes investment casting moulds. *CIRP J Manuf Sci Tech* 13: 97–103
20. Harun Z, Kamarudin NH, Ibrahim M, Idris MI, Ahmad S (2015) Reinforced green ceramic shell mould for investment casting process. *Adv Mater Res* 1087:415–419
21. Youmoué M, Téné Fongang RT, Sofack JC, Kamseu E, Chinje Melo U, Tonle IK, Leonelli C, Rossignol S (2017) Design of ceramic filters using clay/sawdust composites: effect of pore network on the hydraulic permeability. *Ceram Int* 43(5):4496–4507
22. Sales A, Rodrigues de Souza F, Almeid FDCR (2011) Mechanical properties of concrete produced with a composite of water treatment sludge and sawdust. *Constr Build Mater* 25: 2793–2798
23. Islam MN, Islam MS (2011) Mechanical properties of chemically treated sawdust-reinforced recycled polyethylene composites. *Industrial Engg Chem Research* 50:11124–11129
24. Duan P, Yan C, Zhou W, Luo W (2016) Fresh properties, mechanical strength and microstructure of fly ash geopolymer paste reinforced with sawdust. *Constr Build Mater* 111:600–610
25. Pattnaik SR, Karunakar DB, Jha PK (2012) Influence of injection process parameters on dimensional stability of wax patterns made by the lost wax process using Taguchi approach. *P I Mech Eng L- J Mater Design Appl* 227(1):52–60
26. Sidhu BS, Kumar P, Mishra BK (2008) Effect of slurry composition on plate weight in ceramic shell investment casting. *J Mater Engg Performance* 17:489–498
27. Azzam A, Li W (2014) An experimental investigation on the three-point bending behavior of composite laminate. *IOP Conf Series: Materials Science and Engineering* 62 (2014) 012016 doi:10.1088/1757-899X/62/1/012016.
28. Berger MB (2010). The importance and testing of density/porosity/permeability/pore size for refractories. In: Proceedings of the Southern African Institute of Mining and Metallurgy Refractories Conference, pp. 101–116
29. Amira S, Dube D, Tremblay R (2011) Method to determine hot permeability and strength of ceramic shell moulds. *J Mater Process Tech* 211:1336–1340

30. Francois Batllo Viers DS, Mosher JS (2009) Method of improving the removal of investment casting shells. US Patent, US7503379 B2.
31. Pattnaik SR, Jha PK, Karunakar DB (2015) A novel method of increasing ceramic shell permeability and optimizing casting shrinkage and tensile strength of the investment cast parts. P I Mech Eng B- J Engineering Manufacture DOI. doi:[10.1177/0954405415606386](https://doi.org/10.1177/0954405415606386)
32. Kumar S, Kumar P, Shan H.S. (2008). Effect of process parameters on impact strength of Al-7% Si alloy castings produced by VAEPC process. Int J Adv Manuf Technol 38, 586–593, DOI: [10.1007/s00170-007-1197-3](https://doi.org/10.1007/s00170-007-1197-3).
33. Wilding MA (1995) Introduction: the structure of fibres. Chapter, Chemistry of the textiles industry, Page 6, DOI: [10.1007/978-94-011-0595-8_1](https://doi.org/10.1007/978-94-011-0595-8_1), Springer Netherlands
34. Batllo Francois (2003) Method of improving the removal of investment casting shells. US Patent, WO2004062835 A2
35. Lilholt H, Lawther JM (2000). Natural organic fibers. Chapter 1.10, Comprehensive composite materials, Elsevier Publisher 1: (ISBN: 0–080437192); 303–325.